Semiclassical theory for the Maslov-type wave packet: Hierarchy below the semiclassical Feynman kernel

Atsuko Inoue-Ushiyama
Graduate School of Human Informatics, Nagoya University, 464-8601 Nagoya, Japan

Kazuo Takatsuka*
Department of Basic Science, Graduate School of Arts and Sciences, The University of Tokyo, 153-8902 Komaba, Tokyo, Japan
(Received 8 September 1998)

A semiclassical theory based on the Maslov-type wave packet is reported. The present approximation constitutes a class of semiclassical theory that brings about a hierarchy of theoretical structures below or equivalent to the standard semiclassical approximation to the Feynman kernel. We first propose a semiclassical wave function; that is, what we call the action-decomposed function (ADF). An ADF is propagated in time semiclassically along a ''single action surface,'' which is characterized in terms of a given initial momentum, with the phase being proportional to the $F_2(q,p)$-type generating function. An arbitrary wave function can be expanded continuously in the ADF's of different initial momenta, each of which is associated with weighting factors both in configuration and momentum spaces. Depending on the form of the weighting function, the present scheme covers a number of different levels of approximation, ranging from a ''single'' ADF to a semiclassical kernel. Thus our theory provides a way of connecting the Maslov-type semiclassical wave packet to the WKB theory based on the Feynman kernel. It is generally concluded that the above kernel limit attains the highest accuracy possible within the present scheme, but it requires a large number of classical trajectories to represent it. On the other hand, a single ADF yields a little less accurate results but demands the fewest representing classical trajectories due to the narrowest momentum distribution. In fact, we show numerically that the autocorrelation function represented in terms of a single ADF, from which the energy spectrum is extracted with a Fourier transformation, can be calculated with drastically fewer classical trajectories without losing much accuracy. We also present a limitation in applying the ADF, and show an interesting symptom arising from a pathological use of the approximation. The present theory is quite promising for a spectral analysis of the vibrational states of relatively large molecules, if applied appropriately.
[S1050-2947(99)10005-2]

PACS number(s): 03.65.Sq, 03.65.Ge, 31.15.Gy

I. INTRODUCTION

Semiclassical mechanics is not simply an academic problem, but one that covers quite an important and wide domain of research for systems whose nature in between classical and quantum mechanics [1–5]. Such transitions from quantum to classical nature are frequently observed in systems where the Planck constant is relatively smaller than the action integrals characterizing the wavelength of a matter wave for a system. Nuclear dynamics, such as in molecular vibration and chemical reactions, are typical examples. It is also generally believed that an increase of the number of consisting particles is another route from quantum to classical domains in that only the particle nature could survive through the random phase cancellation of associated matter waves [6]. Again, the dynamics of molecular systems, particularly of a large molecular system, can be a prototype. Therefore, in certain dynamics of molecules consisting of many heavy atoms, two routes from quantum to classical mechanics can cross over. We are interested in this interaction between the two limiting stages $\hbar \to 0$ and $N \to \infty$, and its effects on molecular dynamics. Keeping this particular aspect in mind, here we would like to present an interesting kind of semiclassical theory.

As is well known, WKB (Wentzel-Kramers-Brillouin) theory gives the very first step in semiclassical mechanics. Both the asymptotic theory to a wave function [7,8] in the first order of the Planck constant, and that for the Feynman kernel [1,2], are commonly called the WKB theory. (Strictly speaking, they can be different from each other, as will be seen below.) Generally speaking, a higher-order evaluation of the kernel, as in uniform approximations [2,4,5], or an attempt at solutions of the higher hierarchical equations in the Maslov semiclassical theory [3], are definitely among the most desirable tasks in this field. On the other hand, however, more accurate solutions generally demand a higher price of labor. In a marked contrast to the mainstream of semiclassical theory, we develop a semiclassical theory which is in a hierarchical stage below or equal to the standard WKB theory [9]. This kind of study is worth accomplishing if the lower level approximations thus developed can represent a wave function and/or spectrum with far fewer classical trajectories without losing much accuracy. The present property is quite useful in applications to large systems, since it is still difficult to apply even the standard semiclassical kernel to a system of more than, say, three dimensions, let alone the above-mentioned higher-order approximations. In fact we show numerically that this is cer-

*Author to whom correspondence should be addressed. Electronic address: KazTak@mns2.c.u-tokyo.ac.jp

tainly the case: Our proposed semiclassical approximation indeed reproduces reasonably accurate spectra of molecular vibrations with far fewer classical trajectories than the semiclassical Feynman kernel.

We first investigate a semiclassical wave function, what we call the action-decomposed function (ADF). An ADF propagates in time semiclassically only along a single action surface that is characterized in terms of an $F_2(q,p_0)$-type generating function [10], which specifies the initial momentum p_0 everywhere in configuration space. An arbitrary wave function can be represented continuously in ADF's of different initial momenta. The wave function thus represented is equipped internally with weighting functions both in configuration and momentum spaces. Depending on the form of the weighting functions, the present scheme covers a number of different levels of approximation, ranging from the semiclassical Feynman kernel to a single ADF approximation, which has a δ-function momentum distribution. In this way, we have a new route connecting the Maslov semiclassical theory with the WKB theory based on the Feynman kernel. (It is well known that the Van Vleck transformation theory [11,12] for a wave packet produces essentially the same propagation as the semiclassical Feynman kernel.) It is anticipated that the above kernel limit should attain the highest accuracy possible within the present scheme. On the other hand, a single ADF in turn would yield slightly less accurate results, but requires the fewest representing classical trajectories because of the narrowest momentum distribution. In fact we show that the number of trajectories required to represent the autocorrelation function in terms of a single ADF can be drastically reduced without losing much accuracy by using a single ADF.

Another, but less practical, advantage to exploring the lower hierarchical structure below the standard semiclassical theory is that some insight into quantum-classical correspondence is deepened. For instance, an inappropriate application of the ADF can miss taking account of some interference effects of quantum phases. We present such an example, in which a negative-energy spectrum is generated for a positive potential system. (This erratic situation is closely related to the general role of phase destructive interference, and hence will be studied in great detail in a companion paper.) We thus clarify the limitation in applying the ADF. With this note in mind in practical applications, the present theory is quite promising for a spectral analysis of the vibrational states of relatively large molecules.

The present paper is organized as follows. In Sec. II, after the standard semiclassical approximation of the Feynman kernel is briefly reviewed, we discuss a semiclassical framework based on the Maslov-type wave packet, and present an explicit form of the ADF. Section III describes how a general wave function can be represented and propagated in terms of the action-decomposed functions, the most expensive extreme of which is equivalent to propagation based on the Feynman kernel. We then show numerically in Sec. IV how a single action-decomposed function can actually work. In Sec. V we discuss qualitative conditions for the ADF to be a good semiclassical approximation.

II. SEMICLASSICAL DYNAMICS FOR THE ACTION-DECOMPOSED FUNCTION (ADF)

We consider a semiclassical representation for a wave function directly, rather than that for the Feynman kernel. In view of its generality and popularity, however, it is convenient to begin by reviewing the semiclassical kernel briefly.

A. Semiclassical Feynman kernel

We begin with a primitive semiclassical expression for $K(q,q_0;t)=\langle q|\exp[-(i/\hbar)Ht]|q_0\rangle$; that is,

$$K^{\rm sc}(q,q_0;t)=(2\pi i\hbar)^{-N/2}\left|\frac{\partial q}{\partial p_0}\right|^{-1/2} \times\exp\left[\frac{i}{\hbar}S_1(q,q_0;t)-\frac{i\pi\mu}{2}\right], \qquad (2.1)$$

where q and q_0 are given points in configuration space that are to be connected by classical paths [1,2]. [It is understood implicitly throughout the present paper that when more than one classical path connects q_0 and q, all those contributions should be summed up coherently in Eq. (2.1).] $S_1(q,q_0;t)$ is an action integral for this path, and μ is the Maslov index in this representation. N denotes the dimension of configuration space. As is well known, the above straightforward asymptotic approximation of the kernel breaks down at caustic points where the amplitude factor diverges: $|\partial q/\partial p_0|^{-1/2}=\infty$. In the 1990s, a general scheme to avoid singularities at caustics without resorting to tedious uniform approximations [2,4] has been developed by several authors independently [13]. Among various possible forms, the initial value representation [13(a)]

$$K^{\rm sc}(q,q_0;t)=(2\pi i\hbar)^{-N/2}\int dp_0\,\delta(q-q_t)\left|\frac{\partial q_t}{\partial p_0}\right|^{1/2} \times\exp\left[\frac{i}{\hbar}S_1(q_t,q_0;t)-\frac{i\pi\mu}{2}\right] \qquad (2.2)$$

gives an elegant example. Note, that, in this expression, q_t is specified as the end point in configuration space at time t of a classical trajectory starting from (q_0,p_0) in phase space, and therefore the root-search procedure inherent to Eq. (2.1) is not needed. The explicit divergence in the amplitude factor of Eq. (2.1) has been removed through a transformation of integral variable from q_t to p_0. The new amplitude factor $|\partial q_t/\partial p_0|^{1/2}$ becomes only zero at the caustic points.

With Eq. (2.2), a semiclassical wave function is obtained in double integrals such that

$$\Psi(q,t)=\int dq_0\,K^{\rm sc}(q,q_0;t)\Psi(q_0,0) =(2\pi i\hbar)^{-N/2}\int\int dp_0\,dq_0\,\delta(q-q_t)\left|\frac{\partial q_t}{\partial p_0}\right|^{1/2} \times\exp\left[\frac{i}{\hbar}S_1(q_t,q_0;t)-\frac{i\pi\mu}{2}\right]\Psi(q_0,0), \qquad (2.3)$$

and the autocorrelation function, the Fourier transform of which gives the energy spectrum, is again represented in a double integral due to the presence of the δ function in Eq. (2.3), such that

$$C(t)=\int dq\,\Psi^*(q,0)\Psi(q,t)$$
$$=(2\pi i\hbar)^{-N/2}\int\int dp_0\,dq_0\left|\frac{\partial q_t}{\partial p_0}\right|^{1/2}\Psi^*(q_t,0)\Psi(q_0,0)$$
$$\times\exp\left[\frac{i}{\hbar}S_1(q_t,q_0;t)-\frac{i\pi\mu}{2}\right]. \tag{2.4}$$

Thus this initial value representation turns out to be much easier in use. However, the initial momentum p_0, which has no finite distribution in Eqs. (2.3) and (2.4), should be sampled from the space of infinite size, which results in a very slow convergence in the numerical integration of Eq. (2.4).

Finally, another representation of the semiclassical kernel is appended [13c], since this is more relevant to our theoretical development which is mainly described in the (q_t,p_0) representation. The kernel $K(q,p_0;t)=\langle q|\exp[-(i/\hbar)Ht]|p_0\rangle$ has its semiclassical counterpart

$$K^{\rm sc}(q,p_0;t)=(2\pi i\hbar)^{-N/2}\int dq_0\,\delta(q-q_t)\left|\frac{\partial q_t}{\partial q_0}\right|^{1/2}$$
$$\times\exp\left[\frac{i}{\hbar}S_2(q_t,p_0;t)-\frac{i\pi M}{2}\right]. \tag{2.5}$$

The Maslov index M arises from the sign change of $\partial q_t/\partial q_0$. This kernel works on the momentum representation of an initial wave function $(\tilde{\Psi}(p_0,0))$ such that

$$\Psi(q,t)=(2\pi i\hbar)^{-N/2}\int\int dp_0\,dq_0\,\delta(q-q_t)\left|\frac{\partial q_t}{\partial q_0}\right|^{1/2}$$
$$\times\exp\left[\frac{i}{\hbar}S_2(q,p_0;t)-\frac{i\pi M}{2}\right]\tilde{\Psi}(p_0,0). \tag{2.6}$$

This form shows up later as a special case of our semiclassical wave functions.

B. Equations of motion for a wave packet

We now turn from the kernel to a wave packet. Maslov and Feodoriuk established a systematic theory to generate a class of wave functions beginning with a form [3]

$$\Psi(q,t)=F(q,t)\exp\left[\frac{i}{\hbar}S_{\rm cl}\right], \tag{2.7}$$

where $S_{\rm cl}$ denotes the classical action satisfying the Hamilton-Jacobi equation

$$\frac{\partial S_{\rm cl}}{\partial t}+H\left(q,\frac{\partial S_{\rm cl}}{\partial q},t\right)=0. \tag{2.8}$$

Unlike the Bohm formalism [14], the exponential part is fixed to be the purely classical action, and therefore no ''quantum potential'' arises. Instead, the amplitude function F in Eq. (2.7) is to be asymptotically expanded in terms of $\lambda^{-1}=\hbar/2\pi i$, giving rise to a hierarchical transport equation for each order of λ^{-1} (or $\hbar$) [3]. The physical meaning of the higher-order terms is not necessarily clear, however. It is easy to see $F(q,t)$ satisfying the simple equation of motion

$$\frac{\partial F}{\partial t}+\nu\cdot\nabla F+\frac{1}{2}(\nabla\cdot\nu)F=\frac{i\hbar}{2}\nabla^2F, \tag{2.9}$$

where ν is the classical velocity defined as $\nu=\partial S_{\rm cl}/\partial q$. The mass-weighted coordinates are used throughout so that all the masses are scaled to unity. In the limit of $\hbar\to0$, Eq. (2.9) corresponds to the lowest-order transport equation

$$\frac{\partial F}{\partial t}+\nu\cdot\nabla F+\frac{1}{2}(\nabla\cdot\nu)F=0. \tag{2.10}$$

From this equation and its complex-conjugate counterpart, the following equation of continuity follows:

$$\frac{\partial(FF^*)}{\partial t}+\nabla\cdot(\nu FF^*)=0. \tag{2.11}$$

Since FF^* represents the density of classical particles in configuration space moving along the classical velocity field $\nu(q,t)=\partial S_{\rm cl}/\partial q$, $F(q_t,t)$ gives a ''complex-valued classical flow,'' which is termed as the WKB flow.

Defining a substantial time derivative along the flow such that

$$\frac{D}{Dt}\equiv\frac{\partial}{\partial t}+\nu\cdot\nabla+\frac{1}{2}\nabla\cdot\nu, \tag{2.12}$$

one can rewrite Eq. (2.9) as

$$\frac{DF}{Dt}=\frac{i\hbar}{2}\nabla^2F. \tag{2.13}$$

This is nothing but a diffusion equation with an imaginary diffusion constant $i\hbar/2$. The diffusion takes place not in a simple homogeneous space but on the WKB flow, in other words, diffusing points jump from one classical flow line to another. In this way, the higher-order effects can be taken into account without resorting to the hierarchical transport equations due to Maslov and Feodoriuk [3]. Although extremely interesting, this aspect will be studied in our future publications.

We come back to the lowest semiclassical approximation [Eq. (2.10)], writing down its explicit solution [9]. A formal solution to Eq. (2.10) is given by an exponential form $F(q(t))=F(q(0))\exp[-\int_0^t\nabla\cdot\nu/2]$, which, however, breaks down at caustics.

C. Explicit solution to the equation of motion—action-decomposed function

We now present an explicit solution satisfying an appropriate initial condition to Eq. (2.10). From this equation, one can also derive an equation of motion for F^2 (besides that for $|F|^2$)

$$\frac{\partial F^2}{\partial t}+\boldsymbol{\nabla}\cdot(\nu F^2)=0. \tag{2.14}$$

Notice here that $F(q,t)$ can take an imaginary value, and hence F^2 can be negative. F^2 can be readily integrated locally along a classical path in terms of a quantity $(\partial q_t/\partial q_0)^{-1}$, since by taking partial derivatives of the Hamilton-Jacobi equation for $S_{\rm cl}(q,p_0;t)$ in terms of p_0 and q successively, we have a similar equation to Eq. (2.14), that is,

$$\frac{\partial}{\partial t}\left(\frac{\partial q_t}{\partial q_0}\right)^{-1}+\boldsymbol{\nabla}\cdot\left[\nu\left(\frac{\partial q_t}{\partial q_0}\right)^{-1}\right]=0. \tag{2.15}$$

Furthermore, one has a trivial initial condition $(\partial q_t/\partial q_0)^{-1}=1$, since $q_t=q_0$ at $t=0$, indicating that $(\partial q_t/\partial q_0)^{-1}$ can be regarded as a local representation of the Green function of Eq. (2.14). On comparing Eqs. (2.14) and (2.15), together with the initial conditions above, one immediately has [9]

$$\begin{aligned}F(q_t,t)&=F(q_0,0)\left(\frac{\partial q_t}{\partial q_0}\right)^{-1/2}\\&=F(q_0,0)\left|\frac{\partial q_t}{\partial q_0}\right|^{-1/2}\exp\left[-\frac{i\pi M}{2}\right],\end{aligned} \tag{2.16}$$

where the derivative $\partial q_t/\partial q_0$ is taken under the fixed initial momentum p_0, and M is the Maslov index in this representation that counts the number of zeros of $\partial q_t/\partial q_0$ up to degeneracy. $\partial q_t/\partial q_0$ is a minor determinant arising from the so-called stability matrix [1,4,5,15]

$$\frac{\partial Z_t}{\partial Z_0}=\begin{pmatrix}\dfrac{\partial q_t}{\partial q_0} & \dfrac{\partial q_t}{\partial p_0}\\ \dfrac{\partial p_t}{\partial q_0} & \dfrac{\partial p_t}{\partial p_0}\end{pmatrix}, \tag{2.17}$$

and $(\partial q_t/\partial q_0)^{-1}=\partial^2 S_{\rm cl}(q_t,p_0;t)/(\partial q_t\partial p_0)$ is interpreted as the density of the families of classical paths having a common initial momentum p_0.

With the above choice of the initial condition, the classical action in Eq. (2.7) is naturally fixed to the F_2-type generating function of Goldstein [10], namely,

$$S_{\rm cl}(q,p_0;t)=F_2(q,p_0;t)=F_1(q,q_0;t)+q_0p_0. \tag{2.18}$$

[The generating functions F_1 and F_2 should not be confused with our amplitude function $F(q,t)$.] In other words, all the classical paths representing Eq. (2.7) lie commonly on a single action surface, the initial momentum of which is p_0 everywhere. We therefore term this function as an ADF. Having the F_2 generating function as a phase, the initial form of the ADF at $t=0$ is rewritten as

$$\Psi_{p_0}(q,t)=F(q,0)\exp\left[\frac{i}{\hbar}p_0q\right]. \tag{2.19}$$

There is a family of wave functions that have the form of Eq. (2.19), with a typical example being the coherent state [2,16], in which $F(q,0)$ is a Gaussian function (see also Ref. [17] for Heller's Gaussian approach).

A wave function which consists of a single ADF, denoted by $\Psi^{p_0}_{\rm local}(q_t,t)$, is specified as a single ADF (SADF). Since a SADF is given at the end points of classical trajectories, one may want to rewrite it in a slightly more global form as

$$\begin{aligned}\Psi_{p_0}(q,t)&=\int dq_t\,\delta(q-q_t(q_0,p_0))\Psi^{p_0}_{\rm local}(q_t,t)\\&=\int dq_0\,\delta(q-q_t(q_0,p_0))\Psi^{p_0}_{\rm local}(q_t,t)\left|\frac{\partial q_t}{\partial q_0}\right|\\&=\int dq_0\,\delta(q-q_t(q_0,p_0))F(q_0,0)\left|\frac{\partial q_t}{\partial q_0}\right|^{1/2}\\&\quad\times\exp\left[\frac{i}{\hbar}S_2(q_t,p_0;t)-\frac{i\pi M}{2}\right].\end{aligned} \tag{2.20}$$

Although the local solution $F(q_t,t)$ in Eq. (2.16) diverges at every caustic point where the Jacobian determinant $\partial q_t/\partial q_0$ becomes zero, the global solution Eq. (2.20) does not suffer from such a divergence. This is again due to the transformation of the integral variable from q_t to q_0 [13].

Note that the action-decomposed function in Eq. (2.20) is represented in terms of N-dimensional integration over the initial coordinate q_0, which should be compared with Eq. (2.3), in which $2N$ integrations over p_0 and q_0 are required. Likewise, the autocorrelation function is written with a SADF such that

$$\begin{aligned}C(t)&=\langle\Psi_{p_0}(0)|\Psi_{p_0}(t)\rangle\\&=\int dq_0\,F^*(q_t,0)F(q_0,0)\left|\frac{\partial q_t}{\partial q_0}\right|^{1/2}\\&\quad\times\exp\left[-\frac{i}{\hbar}p_0q_t+\frac{i}{\hbar}S_2(q_t,p_0;t)-\frac{i\pi M}{2}\right],\end{aligned} \tag{2.21}$$

which is also an N-dimensional integral, while that of Eq. (2.4) is $2N$ dimensional. Therefore it is anticipated that the correlation function of Eq. (2.21) and its deduced spectra may be extracted with much fewer classical trajectories. It is thus the main aim of the rest of the present paper to demonstrate that this is really the case.

D. Orthogonal property of the action-decomposed functions

Before a numerical examination of an ADF, we touch upon a weak (semiclassical) orthogonality among the ADF's. SADF's that are characterized by different initial momenta are orthonormalized to each other in the lowest-order approximation of $\hbar$, such that

$$\int \Psi^*_{p_i}(q,t)\Psi_{p_j}(q,t)dq=\begin{cases}1 & \text{if } p_i=p_j,\\ O(\hbar^N) & \text{otherwise.}\end{cases} \tag{2.22}$$

A proof for Eq. (2.22) is given in the Appendix. [The proof assumes that the amplitude function $F(q,t)$ is smooth enough, but the resultant orthogonality expression does not depend on the practical form of $F(q,t)$, as far as the Planck constant is small enough.] This fact suggests taking a set of ADF's as a basis to expand any wave function. However, unlike the case of the coherent state representation [2,16], we do not have a resolution of the identity in terms of a continuous momentum parameter p, nor even a (over)completeness relation.

Effectively, however, a discretized representation can be constructed as follows. Let us reformulate the above normalization such that

$$\int \Psi^*_{p_i}(q,t)\Psi_{p_j}(q,t)dq=\begin{cases}\dfrac{1}{w_i} & \text{if } p_i=p_j,\\ O(\hbar) & \text{otherwise,}\end{cases} \tag{2.23}$$

where the momenta are chosen at the quadrature points, and w_i are the weighting factors at these points [18]. Then, we can set an effective resolution of identity

$$\sum_i w_i|\Psi_{p_i}(t)\rangle\langle\Psi_{p_i}(t)|\cong 1, \tag{2.24}$$

since we have

$$\left(\sum_i w_i|\Psi_{p_i}(t)\rangle\langle\Psi_{p_i}(t)|\right)\left(\sum_j w_j|\Psi_{p_j}(t)\rangle\langle\Psi_{p_j}(t)|\right)$$
$$\cong\left(\sum_i w_i|\Psi_{p_i}(t)\rangle\langle\Psi_{p_i}(t)|\right), \tag{2.25}$$

and hence, for an arbitrary function $|f\rangle$, it holds that

$$|f\rangle\approx\left(\sum_i w_i|\Psi_{p_i}(0)\rangle\langle\Psi_{p_i}(0)|\right)|f\rangle$$
$$\cong\int dp_i|\Psi_{p_i}(0)\rangle\langle\Psi_{p_i}(0)|f\rangle. \tag{2.26}$$

Thus $|f\rangle$ can be approximately evolved in time with $|\Psi_{p_i}(t)\rangle$, under Eq. (2.26), the coefficient of which is $w_i\langle\Psi_{p_i}(0)|f\rangle$.

III. REPRESENTATION OF A WAVE FUNCTION IN TERMS OF ADF

In Eq. (2.26), we have shown how an arbitrary wave function can be propagated in terms of ADF's. In this section, we take another approach to utilizing the ADF, which will clarify a relationship between our semiclassical scheme and that of the Feynman kernel, thereby characterizing more clearly about a hierarchical structure of the semiclassical theory down to classical mechanics.

Suppose we have a decomposition for an arbitrary wave function such that

$$\Psi(q)=F(q)G(q), \tag{3.1}$$

under a condition that $G(q)$ has a momentum representation

$$\tilde{G}(p)=\frac{1}{(2\pi\hbar)^N}\int G(q)\exp\left(-\frac{i}{\hbar}pq\right)dq. \tag{3.2}$$

We assume that $F(q)$ is a slowly varying function in q space, while $G(q)$ is (relatively) oscillatory function like a plane wave. There is no uniqueness in this decomposition though. Nonetheless, we will show that the theory works well enough if the Planck constant is small. The total wave function thus decomposed is rewritten as

$$\Psi(q)=\int dp_0\,\tilde{G}(p_0)F(q)\exp\left(\frac{i}{\hbar}p_0q\right), \tag{3.3}$$

in which one recognizes the initial form of ADF that appeared in Eq. (2.19). Hence we now have another way of propagating a general wave function, where $\tilde{G}(p)$ is regarded as a weighting function in momentum space. The semiclassical time propagation of this wave function is straightforward with use of Eq. (2.20), that is,

$$\Psi(q,t)=\int\int dq_0\,dp_0\,\delta(q-q_t)\left|\frac{\partial q_t}{\partial q_0}\right|^{1/2}F(q_0,0)\tilde{G}(p_0)$$
$$\times\exp\left(\frac{i}{\hbar}S_2(q_t,p_0;t)-\frac{i\pi M}{2}\right), \tag{3.4}$$

where $q_0=\partial S_2(q,p_0,t=0)/\partial p_0$. There has been no need to assume the completeness of the ADF in this representation. This wave function materializes a semiclassical way of phase-space representation of a quantum wave function (see Refs. [15,19] and references cited therein for a phase-space representation of quantum mechanics). It is straightforward to see that the form of Eq. (3.4) holds also for $t=0$, which is brought back to Eq. (3.3). Let us show some simple examples of the above decomposition and their consequences.

(1) SADF. Setting

$$F=F(q)\quad\text{and}\quad G=\exp\left(\frac{i}{\hbar}p_0q\right) \tag{3.5}$$

at $t=0$, we have

$$\tilde{G}(p)=\delta(p-p_0) \tag{3.6}$$

and

$$\Psi(q,0)=F(q)\exp\left(\frac{i}{\hbar}S_2(q,p_0;0)\right)$$
$$=F(q)\exp\left(\frac{i}{\hbar}p_0 q\right), \tag{3.7}$$

which is just a SADF.

(2) *The semiclassical kernel* $K(q_t,p_0;t)$. Set

$$F(q)=1 \quad \text{(const)},$$
$$G(q)=\Psi(q) \quad \text{(wave function itself)}, \tag{3.8}$$

with

$$\tilde{G}(p)=\tilde{\Psi}(p) \quad \text{(momentum representation of the wave function)} \tag{3.9}$$

and we have

$$\Psi(q,t)=(2\pi\hbar)^{-N}\int\int dq_0\,dp_0\,\delta(q-q_t)\left|\frac{\partial q_t}{\partial q_0}\right|^{1/2}\exp\left(\frac{i}{\hbar}S_2(q_t,p_0;t)-\frac{i\pi M}{2}\right)\tilde{\Psi}(p_0). \tag{3.10}$$

Comparison of this expression with Eq. (2.6) shows that Eq. (3.10) is essentially the same as a wave function propagated with the kernel $K^{sc}(q_t,p_0;t)$ (aside from a minor difference in the coefficients), that is,

$$\Psi(q,t)=\int dp_0\,K^{sc}(q,p_0;t)\tilde{\Psi}(p_0,0). \tag{3.11}$$

Thus we have found another relation of the Maslov-type wave packet to the Feynman kernel in a semiclassical stage. However, there can exist many different choices in the decomposition of Eq. (3.1), which constitute a lower hierarchy below the kernel limit. Finally, we note an important technical difference between the kernel-type propagation [Eq. (3.10)] and that of a SADF [Eq. (2.20)]. It is obvious that Eq. (2.20) requires only N-fold integration, while the integral of Eq. (3.10) consists of $2N$ variables. In addition, Eq. (3.10) employs the momentum representation of a wave function, which requires N more integrals unless $\tilde{\Psi}(p_0)$ can be obtained analytically.

IV. NUMERICAL STUDY ON CORRELATION FUNCTION AND SPECTRA

In this section we numerically examine the accuracy and tractability of our semiclassical scheme by applying it to the autocorrelation function and its Fourier (energy) spectrum. A variety of decompositions of a wave function, ranging from the kernel limit to a SADF, are tested with different system parameters such as the magnitude of the Planck constant and the anharmonicity. Emphasis is placed on the convergence of the correlation function and spectra with respect to the number of sampled trajectories.

A. Area of sampling space to apply ADF

The accuracy and convergence property of the semiclassical propagation depend on the decomposition of Eq. (3.1). Here we study the effect of the decomposition systematically by choosing a Gaussian function as an initial wave function,

$$\Psi(q)=\left(\frac{\pi}{a+b}\right)^{1/4}\exp\left(-(a+b)(q-q_c)^2+\frac{i}{\hbar}p_c(q-q_c)\right), \tag{4.1}$$

which is divided into

$$F(q)=\left(\frac{\pi}{a+b}\right)^{1/4}\exp(-a(q-q_c)^2)$$

and

$$G(q)=\exp\left(-b(q-q_c)^2+\frac{i}{\hbar}p_c(q-q_c)\right), \tag{4.2}$$

with

$$\tilde{G}(p_0)=\frac{1}{(2\pi\hbar)}\left(\frac{\pi}{b}\right)^{1/2}\exp\left[-\frac{1}{4b}\left(\frac{p_0-p_c}{\hbar}\right)^2\right]. \tag{4.3}$$

Thus, an area in the initial sampling phase space (q_0,p_0) representing the propagation must be roughly proportional to

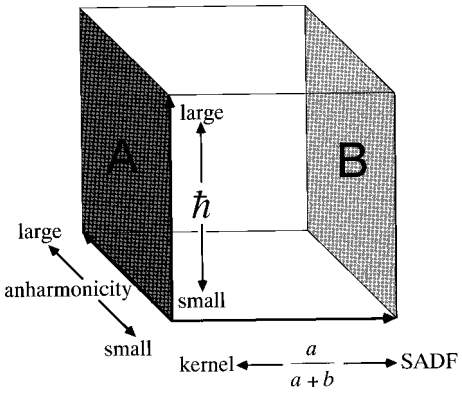

FIG. 1. The schematic picture of the parameter space in which the semiclassical approximations are examined. *A* stands for the semiclassical Feynman kernel, while *B* is dedicated to the SADF. The height represents the magnitude of the Planck constant, and the depth the extent of the anharmonicity of a potential.

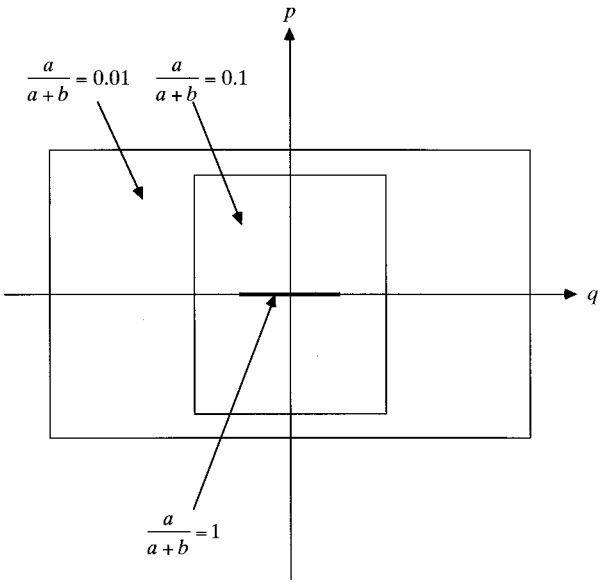

FIG. 2. Schematic picture of the sampling areas in phase space, from which classical trajectories are picked randomly to represent the semiclassical wave functions. The boxes are for $a/(a+b)=1$, 0.1, and 0.01.

$$\left(\frac{b}{a}\hbar^2\right)^{1/2}. \tag{4.4}$$

Fixing $a+b=\frac{1}{2}$, we can parametrize the two extremes, namely, the limits of the kernel and SADF, and general cases in between: (i) The maximum sampling area with $a=0$. As stated above [cf. Eq. (3.8)], this case corresponds to a full use of the Feynman kernel of the form $\Psi(q,t)=\int dp_0\, K^{\rm sc}(q,p_0,t)\tilde{\Psi}(p_0,0)$ as in Eq. (3.10). We therefore call this case the kernel limit. (ii) The minimum sampling space with $b=0$. In this case, $\tilde{G}(p_0)=\delta(p_0-p_c)$, as in Eq. (3.6). This is just the case of a SADF. The initial trajectories are picked so as to have only a given momentum p_c.

B. Test systems

Our test systems are one-dimensional harmonic and Morse oscillators. As a harmonic case we simply use

$$H=\frac{p^2}{2}+\frac{q^2}{2}, \tag{4.5}$$

with an initial wave packet

$$\Psi(q,0)=\left(\frac{1}{\pi}\right)^{1/4}\exp\left(-\frac{1}{2}q^2\right), \tag{4.6}$$

which is an eigenfunction of Eq. (4.5) if $\hbar=1.0$. The following Hamiltonian

$$H=\frac{p^2}{2}+D[1-\exp(-\lambda q)]^2, \tag{4.7}$$

with the parameters $D=30$ and $\lambda=0.08$, is adopted as an anharmonic problem. An initial wave packet is set to

$$\Psi(q,0)=\left(\frac{1}{\pi}\right)^{1/4}\exp\left[-\frac{1}{2}(q-q_c)^2+\frac{i}{\hbar}p_0 q\right], \tag{4.8}$$

located at $q_c=-7$ and $p_0=0$.

The Gaussian quadrature [18] is the most useful to sample the initial phase-space points for carrying out the integration in the one-dimensional case. However, since we are interested in applying the semiclassical scheme to a large system, in which only Monte Carlo type sampling is practical, and since we are studying the rate of convergence with respect to the number of trajectories, we would rather adopt the random-number sampling.

C. Quality of spectra with change of the system parameters

We first examine the quality of the correlation function and its related spectra in the various approximations, using a sufficiently large number of classical trajectories. The convergence property will be investigated in the next subsection. There are three parameters that characterize the system as shown in Fig. 1: (i) The anharmonicity (harmonic or Morse). (ii) The magnitude of the Planck constant ($\hbar=1.0$ or 0.1). (iii) The ratio of b to a specifying the decomposition of Eq. (4.1) in between a SADF and the kernel. Although $\sqrt{b/a}$ is a good parameter to see the convergence property, we also use $a/(a+b)$ to parametrize the quality of approximation. The smaller (larger) this is, the closer the approximation approaches the kernel (SADF) limit, namely, $a/(a+b)=0$ [$a/(a+b)=1$] for the kernel (SADF). Three cases are picked for $a/(a+b)=1.0$, 0.1, and 0.01 in practice, as depicted in Fig. 2, which specifies the sizes of areas in phase space required for sampling. In what follows, we simply denote the case of $a/(a+b)=0.01$ to be the kernel limit. Obviously, the kernel limit is the most tedious, but it is supposed to give the most accurate results (in particular, an exact result for the harmonic potential).

1. Harmonic potential with a large Planck constant—spurious spectrum

We begin with the poorest example, in that the validity of the SADF approximation could be violated. This is a case of a harmonic potential [Eq. (4.5)] with a large Planck constant

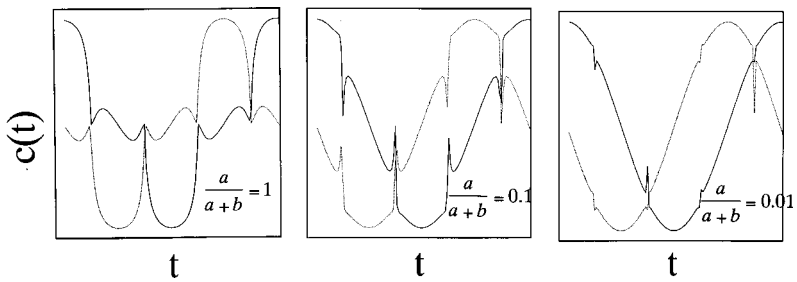

FIG. 3. The autocorrelation function for a harmonic oscillator with $\hbar=1$. The real and imaginary parts are drawn by the solid and dashed lines, respectively. A large deviation between the kernel limit [$a/(a+b)=0.01$] and the SADF [$a/(a+b)=1.0$] is observed.

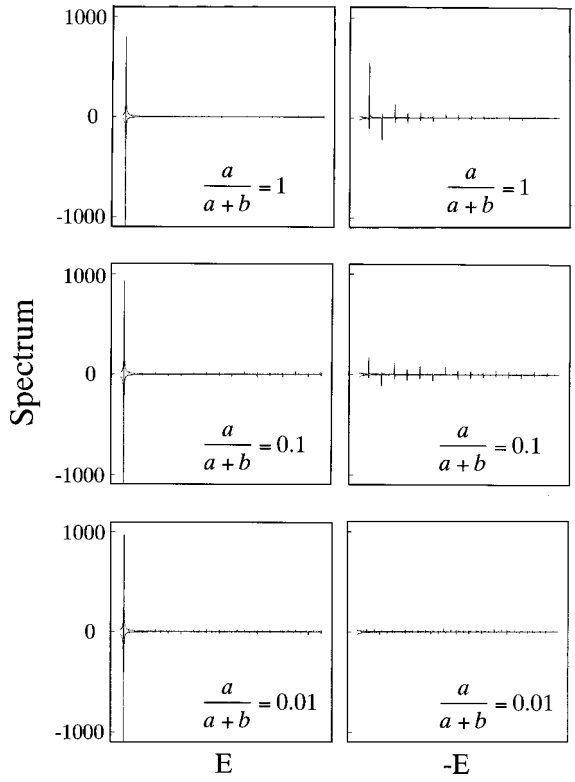

FIG. 4. The positive (left boxes) and negative (right boxes) spectra arising from the harmonic oscillator with $\hbar=1$, which are compared in terms of $a/(a+b)$.

($\hbar=1.0$). The present magnitude of the Planck constant is actually very large, and is far from the domain where a semiclassical approximation is generally valid. Also, it should be noted that a SADF does not give the exact results even for a harmonic case. Conversely, a harmonic oscillator is a tougher problem than an anharmonic one for the SADF scheme, in contrast to the kernel, as will be described below.

Applying the decomposition of Eq. (4.1) with Eq. (3.5) to Eq. (4.6), we make a SADF ($b=0$, $p_c=0$). Figure 3 shows the correlation functions in a time interval $[0,4\pi]$. The solid and dotted curves indicate the real and imaginary parts, respectively, in each box, which in turn correspond to different $a/(a+b)$ (1.0, 0.1, and 0.01). A large deviation between the SADF limit $[a/(a+b)=1]$ and the kernel limit $[a/(a+b)=0.01]$ is observed. The kernel limit is essentially exact except for small kinks numerically formed at $t=\pi/2$, and so on. The resultant energy spectra are shown in Fig. 4. The boxes in the left column show the energy spectra, all of which certainly reproduce the peak at the exact place for the quantum number $n=0$, and no other major peaks are seen. On the other hand, the boxes in the right-hand-side column show spurious components of spectra, which take negative values (negative energies for the positive potential). This symptom reflects the worst condition for the application of a SADF. Nonetheless, the kernel limit does not have such a large contamination.

In the succeeding paper we will examine the reason why such negative energies appear [20]. Here we focus on a consequence of the spurious peaks. Although the negative spectrum can be simply ignored as far as the energy for a one-dimensional system is concerned, this is not the case for

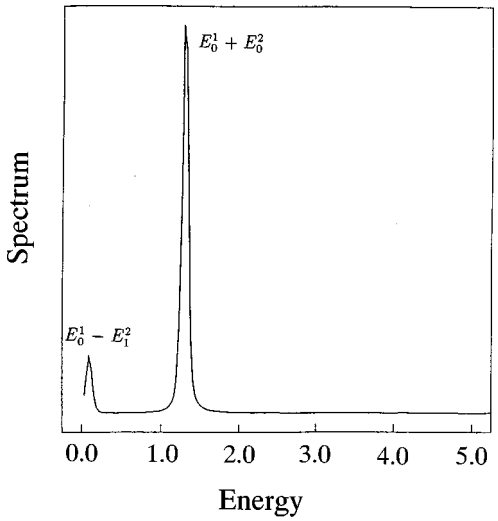

FIG. 5. The power spectrum of a direct product system of two harmonic oscillators with $\hbar=1$. A spurious (subtracting) combination band arises. The energies are in absolute units.

systems greater than or equal to two dimensions. Let us consider a case in which two frequencies are different from each other,

$$H=\left(\frac{p_1^2}{2}+\frac{\omega_1^2 q_1^2}{2}\right)+\left(\frac{p_2^2}{2}+\frac{\omega_2^2 q_2^2}{2}\right) \tag{4.9}$$

with $\omega_1=2$ and $\omega_2=0.6$, and the initial wave packet is prepared as a Gaussian:

$$\Psi_0(q_1,q_2)=\left(\frac{1}{\pi}\right)^{1/2}\exp\left[-\frac{1}{2}(q_1^2+q_2^2)\right]. \tag{4.10}$$

Again, $\hbar=1$. Figure 5 demonstrates that a wrong combination band, namely, a subtracting band $E_0^1-E_1^2$, has appeared as a consequence of the negative spectra. Thus it turns out that a SADF cannot be reliable under this situation.

2. Harmonic potential with a small Planck constant—disappearance of a spurious spectrum

It is quite obvious that such a large Planck constant should deteriorate the quality of the semiclassical approximation, if we look back at Eq. (2.9). With $\hbar=1$ we were simply in a region where the semiclassical approximation is never valid. So let us resume with a smaller choice of the Planck constant at $\hbar=0.1$. With this value, the initial wave function [Eq. (4.6)] is no longer an eigenfunction of the harmonic oscillator. Figure 6 presents a correlation function as in Fig. 3. This time the correlation function for the SADF comes much closer to that of the kernel limit than in the case of $\hbar=1.0$. The spectra are depicted in Fig. 7, the left and right columns corresponding to the positive and negative Fourier spectra, respectively. Note that we have peaks for $n=0,2,4,\ldots$, since Eq. (4.6) is not the eigenfunction of $n=0$. It is clearly observed that the negative components have almost disappeared from the SADF spectrum. Likewise, the

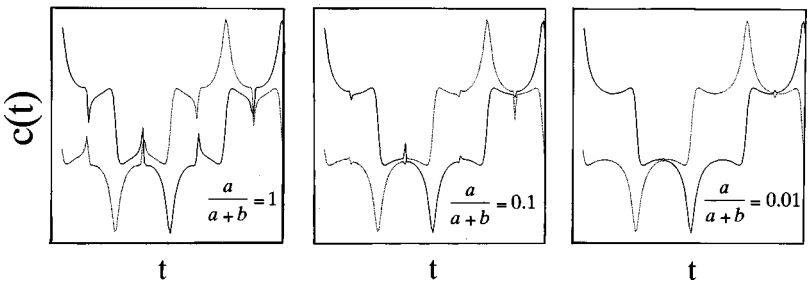

FIG. 6. An autocorrelation function of the harmonic oscillator with $\hbar=0.1$, which should be compared with Fig. 3. The solid and dashed lines are the real and imaginary parts, respectively.

bad (subtracting) combination bands have disappeared from the two-dimensional problem, as shown in Fig. 8. Thus we have confirmed that the smallness of the Planck constant is quite essential for the semiclassical approximation to stay valid.

3. Morse potential with a large Planck constant

It is well known that the semiclassical Feynman kernel gives exact results for harmonic potentials [2], but not for anharmonic systems. This in turn leaves us with an impression that all the semiclassical methods would give less accurate results in anharmonic problems than in harmonic ones. This is not necessarily the case in our semiclassical scheme, as shown below more precisely. The dynamics on a harmonic potential is degenerate [21]; in other words, all the trajectories with different energies (the action variables, more precisely) run collectively with a synchronous phase (the angle variables). Because of this fact, the quantum phase arising from a harmonic oscillator has an extraordinary coherence, which is pathological from the viewpoint of phase cancellation that is expected in more general cases.

As an anharmonic system, we use the Morse oscillator. The Hamiltonian and the initial wave packet are those in Eqs. (4.7) and (4.8). The potential is quite anharmonic around the initial position of the wave packet ($q_c=-7$), where classical trajectories are distributed more widely as the time evolution proceeds. Figure 9 shows the real part of the correlation function from time $t=0$ to 20 (the first row), the energy spectrum in positive values (the second row), and the negative (spurious) energy spectrum (the third row), with the accuracy parameters $[a/(a+b)]$ being 1 (left column) and 0.01 (right column). The Planck constant has been deliberately chosen to be $\hbar=1.0$ despite the pathological results in the harmonic case (Fig. 4). As is observed very clearly, however, even a SADF $[a/(a+b)=1]$ with this large Planck constant gives very good results. For instance, no negative eigenvalues have appeared. The present facts suggest very strongly that the random-phase cancellation due to the nondegenerate motion in phase space for an anharmonic potential can be a very important factor to remove unnecessary spectral components such as the negative spectrum.

Summarizing the results in Secs. IV C 1–IV C 3, we have observed under a condition that $a+b$ in Eq. (4.1) is small enough: (i) The quality of the approximation varies in a continuous manner by changing $a/(a+b)$. (ii) The quality of a SADF significantly deteriorates in the case when a large Planck constant is adopted for a harmonic potential. Nonetheless, it is dramatically improved either if a small Planck constant is used or when an anharmonic potential is considered. There is hence no need to test whether the SADF works well for a nonlinear system with a small Planck constant, which is the case of our primary concern.

D. Convergence with respect to the number of trajectories

We now examine the aspect of computational time. Although the semiclassical approximations below the semiclassical Feynman kernel are not always very accurate, as described above, they demand fewer trajectories to represent wave functions and correlation functions, as shown in Fig. 2 and related mathematical expressions. We now explore how few classical trajectories are required in practice as a function of the parameter $a/(a+b)$. To do this, we check the convergence of the correlation functions with respect to the number of trajectories. The test Hamiltonian and the initial wave packet are again Eqs. (4.7) and (4.8), respectively. Again, three different decompositions, namely $a/(a+b)$

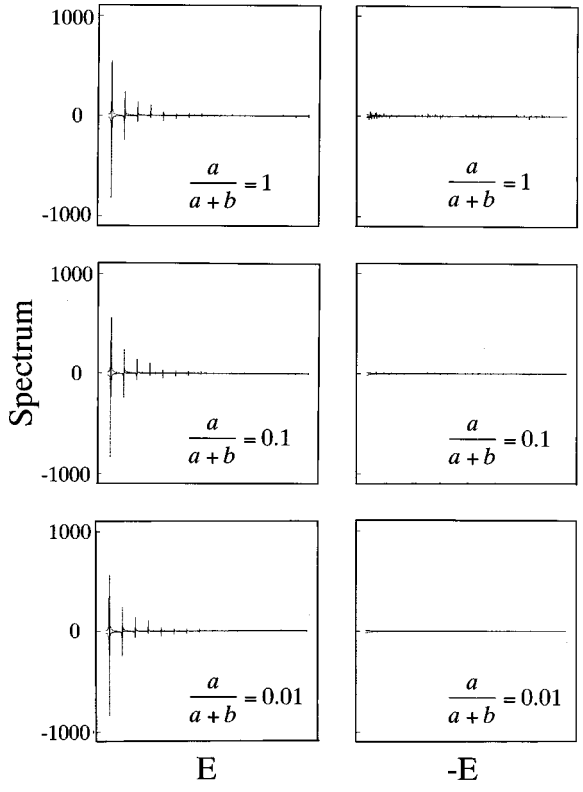

FIG. 7. The positive (left boxes) and negative (right boxes) spectra arising from the harmonic oscillator with $\hbar=0.1$, which should be compared with Fig. 4. The negative components have been virtually removed.

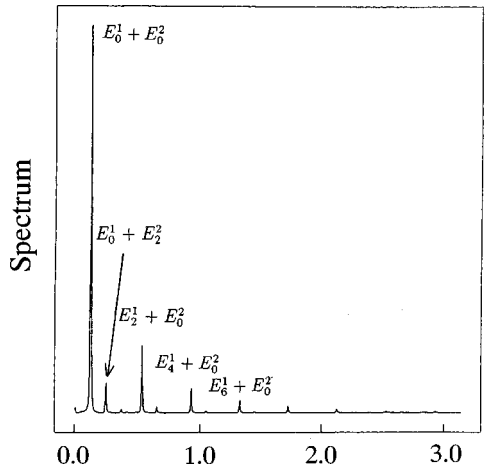

FIG. 8. The power spectrum of a direct product of two harmonic oscillators with $\hbar = 0.1$. No subtracting bands appear. (The small peaks without marks are not the subtracting bands either.)

$=0.01$, 0.1, and 1.0, of a common wave function are employed to calculate the correlation functions. The convergence of the correlation functions is monitored with increasing the number of trajectories. Figure 10 demonstrates a remarkable difference in the convergence: The SADF [panel (a)] needs far fewer trajectories than the kernel limit [panel (c)]. The convergence becomes monotonically slower as we approach the kernel limit.

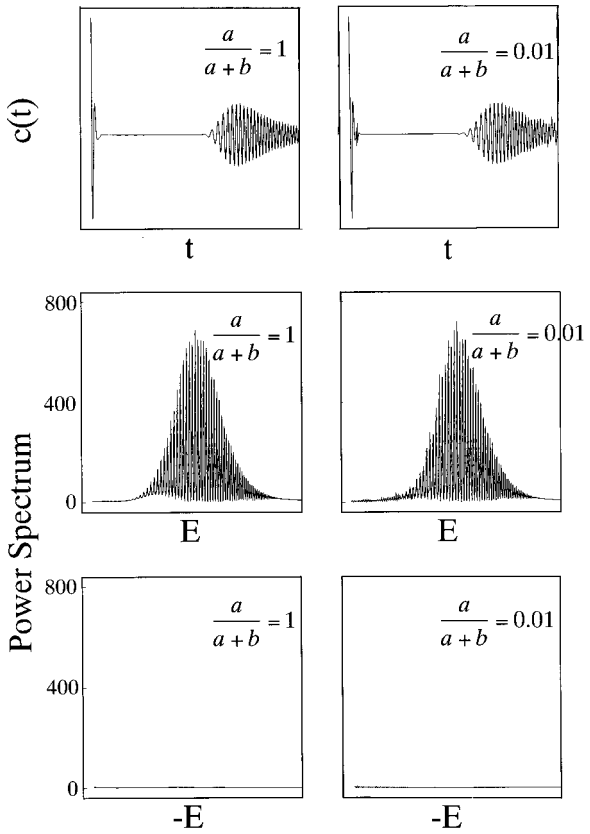

FIG. 9. Comparison of the SADF (left boxes) and the semiclassical kernel (right boxes) in an anharmonic potential. In spite of a large Planck constant ($\hbar = 1$), they yield very similar results. The real parts of the correlation functions (upper row), the positive spectra (middle row), and the negative spectra (lower row) are displayed.

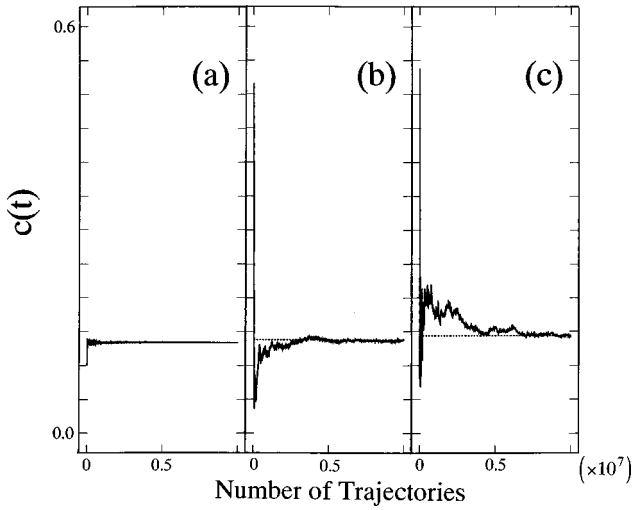

FIG. 10. The rate of convergence of a correlation function represented in ADF's. (a) $a/(a+b) = 1$ (SADF), (b) $a/(a+b) = 0.1$, and (c) $a/(a+b) = 0.01$ (the kernel limit). A dramatic difference in the convergence rate is seen. The absolute values of the correlation functions converged are (a) 0.1340, (b) 0.1375, and (c) 0.1434.

To quantify the rate of convergence more precisely as a function of the decomposition, we consider the convergence rate. First, here we adopt $\sqrt{b/a}$ to specify the decomposition rather than $a/(a+b)$. For the SADF limit $\sqrt{b/a} = 0$, while the kernel limit is located at $\sqrt{b/a} = \infty$. Let us define the convergence ratio as $1.0 - |C(N_{\rm tr})|/|C(\infty)|$, where $|C(N_{\rm tr})|$ is the absolute value of a correlation function fixed at a given parameter $\sqrt{b/a}$ that is calculated with $N_{\rm tr}$ trajectories, and

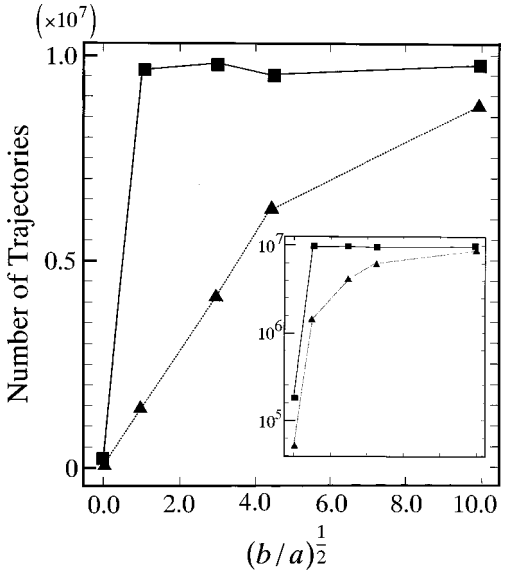

FIG. 11. Number of trajectories to attain the convergence of given percentages as a function of $\sqrt{b/a}$. For instance, the top line indicates the number of trajectories required to have the correlation function converged within 1%. The number of trajectories required to attain this convergence suddenly becomes larger (by about 50 times) by moving from $\sqrt{b/a} = 0$ to $\sqrt{b/a} = 1.0$.

$C(\infty)$ is the corresponding value with practically $N_{\rm tr}=\infty$; for instance, 3% convergence means $|C(N_{\rm tr})|/|C(\infty)|=0.97$. In Fig. 11 we show the number of trajectories required to attain the convergence ratios 1% and 3% versus $\sqrt{b/a}$. The inset of Fig. 11 displays $\log_{10} N_{\rm tr}$ vs $\sqrt{b/a}$. As expected, the number of trajectories required increases almost monotonically as $\sqrt{b/a}$. However, the manner of the increase is not simple. For instance, in the graph for the convergence ratio 1%, a large jump between the case of $\sqrt{b/a}=0$ (SADF) and $\sqrt{b/a}=1.0$ has been observed: The latter needs almost 50 times more trajectories. For a 3% convergence ratio, the kernel limit at $\sqrt{b/a}=10.0$ requires 175 times more trajectories than the SADF. We have thus confirmed and shown the very fast convergence of the SADF, which can be vital to an actual application to large dimensional systems.

V. QUALITATIVE CONDITIONS FOR GOOD ACCURACY IN THE CORRELATION FUNCTION WITH ADF's

Here we deduce qualitative conditions in which the present semiclassical method can work. With use of the general form of the decomposition as in Eq. (3.4), the correlation function is written as

$$C(t)=\int dq\,\Psi^*(q,0)\Psi(q,t)=\int dq_1\,dp_1\int dq_0\,dp_0\,\delta(q_t(q_0,p_0)-q_1)\tilde{G}^*(p_1)\tilde{G}(p_0)F^*(q_1,0)\left|\frac{\partial q_t}{\partial q_0}\right|^{1/2}F(q_0,0)$$
$$\times\exp\left(\frac{i}{\hbar}[S_1(q_t,q_0;t)+q_0p_0-q_1p_1]-\frac{i\pi M}{2}\right). \tag{5.1}$$

First we would like to find what kind of trajectories would dominate this integral, since the present analysis will become necessary later. To do so, we first carry out the integrals over the variables (q_0,p_0), fixing (q_1,p_1). Note, in addition, that the integration should be performed under a constraint

$$q_t(q_0,p_0)=q_1. \tag{5.2}$$

Since the δ function in Eq. (5.1) is not smooth and prevents the stationary phase approximation (SPA) over q_0, we delete it beforehand by integrating over p_0 first. Then the SPA for q_0 leads to

$$\frac{\partial q_t}{\partial q_0}p_t-\frac{\partial q_t}{\partial q_0}p_1=0, \tag{5.3}$$

where we have used Eq. (5.2), and it is

$$p_t=p_1. \tag{5.4}$$

Thus the trajectories making a dominant contribution to the integral should pass through a point, $(q_t(q_0,p_0),p_t(q_0,p_0))=(q_1,p_1)$. The action surface should of course cover this point. Furthermore, in the Fourier transform of the correlation function over the time coordinate, from which the spectra can arise, only a trajectory passing (q_1,p_1) many times can contribute the integral. This is a periodic orbit. Then the integration over (q_1,p_1) requires one to ''sum up'' all the possible periodic orbits, as in the Gutzwiller trace formula [22,23]. The practical differences, however, are (i) we do not analytically reduce the correlation function to a form in which only periodic orbits appear, but carry out the numerical integrations, and (ii) the correlation function in Eq. (5.1) specifies a narrower sampling space due to the factor $\tilde{G}^*(p_1)\tilde{G}(p_0)F^*(q_1,0)F(q_0,0)$.

In case of the SADF, the correlation function is written as

$$C(t)=\int dq_0\,F^*(q_t,0)\left|\frac{\partial q_t}{\partial q_0}\right|^{1/2}F(q_0,0)$$
$$\times\exp\left(\frac{i}{\hbar}[S_1(q_t,q_0;t)+q_0p_0-q_tp_0]-\frac{i\pi M}{2}\right). \tag{5.5}$$

Trajectories dominating this integral can be picked with the use of the stationary phase condition, which leads only to $p_0=p_t$, but no condition between q_0 and q_t arises. Thus not only the periodic orbits but others can contribute to the integral. It is important, however, in view of reducing the error of the correlation function that the stationary phase condition has been satisfied formally, as discussed below.

We next estimate the qualitative errors of the correlation function that employ the ADF's, and thereby figure out what are the conditions for the approximations (including the SADF) to be valid. The error arises from neglecting the term $(i\hbar/2)\nabla^2F(q,t)$ in the equation of motions for $F(q,t)$, Eq. (2.9). Even if $F(q,0)$ is smooth enough [and thereby $\nabla^2F(q,0)$ is very small], $\nabla^2F(q,t)$ is not always small. Therefore we trace how this error is evolved along the WKB flow. From Eq. (2.13), $(DF/Dt)-(i\hbar/2)\nabla^2F$ must be identically zero along the action surface, if F was exact. Thus the evolution of this difference can provide a measure of the error due to the Laplacian term. The first-order error in the correlation function $\Delta C(t)$ can therefore be roughly estimated as

$$\Delta C(t)=-\int dq\,\Psi^*(q,0)\left(\frac{DF}{Dt}-\frac{i\hbar}{2}\nabla^2 F\right)\exp\left(\frac{i}{\hbar}S_{\rm cl}\right)=\frac{i\hbar}{2}\int dq_1\,dp_1\int dq_0\,dp_0\,\delta(q_t(q_0,p_0)-q_1)\tilde{G}^*(p_1)$$
$$\times\tilde{G}(p_0)F^*(q_1,0)[\nabla^2 F(q_t(q_0,p_0),t)]\exp\left(\frac{i}{\hbar}[S_1(q_t,q_0;t)+q_0p_0-q_1p_1]-\frac{i\pi M}{2}\right). \tag{5.6}$$

Here we have used $DF/Dt=0$, that holds for the ADF [see Eq. (2.10)]. This value merely gives an error generated at each time, and the total error should be estimated by accumulating them. Just as in the above procedure leading to Eq. (5.4), one can readily show that this error term is also dominated by the periodic orbits. The contributions from other trajectories are of the magnitude $O(\hbar^{N+1})$. Note that the Laplacian in Eq. (5.6) is now to be operated on the functions of q_t.

Integrating $\Delta C(t)$ in q by parts, and assuming that a wave packet $F(q,t)$ is zero at the asymptotic region ($|q|\to\infty$), we have

$$\Delta C(t)=-\frac{i\hbar}{2}\int dp_1\int dq_t\,dp_0\left|\frac{\partial q_t}{\partial q_0}\right|^{-1}\tilde{G}^*(p_1)\tilde{G}(p_0)\nabla[F^*(q_t,0)]\cdot[\nabla F(q_t(q_0,p_0),t)]\exp\left(\frac{i}{\hbar}\phi\right)$$
$$-\frac{1}{2}\int dp_1\int dq_t\,dp_0\left|\frac{\partial q_t}{\partial q_0}\right|^{-1}\tilde{G}^*(p_1)\tilde{G}(p_0)F^*(q_t,0)[\nabla F(q_t(q_0,p_0),t)]\cdot\nabla[(S_1(q_t,q_0;t)+q_0p_0-q_tp_1)]\exp\left(\frac{i}{\hbar}\phi\right)$$
$$-\frac{i\hbar}{2}\int dp_1\int dq_t\,dp_0\,\tilde{G}^*(p_1)\tilde{G}(p_0)F^*(q_t,0)F(q_t(q_0,p_0),t)$$
$$\times\left[\nabla\left|\frac{\partial q_t}{\partial q_0}\right|^{-1}\right]\cdot\nabla\{[S_1(q_t,q_0;t)+q_0p_0-q_tp_1]\}\exp\left(\frac{i}{\hbar}\phi\right), \tag{5.7}$$

where ϕ denotes the phase part collectively. The error arising from the first term of Eq. (5.7) must be suppressed as long as $\nabla F^*(q_t,0)$ is small enough. Therefore, the initial amplitude function has to be smooth, which is in accord with the above argument when we introduced the decomposition of a wave function into two pieces. Again, however, we note that the flatter $F(q,0)$ is, the more the sampling trajectories are required. The third term of $\Delta C(t)$ can become significant at caustic points where $|\partial q_t/\partial q_0|^{-1}=0$, which is common to all the semiclassical approximations of this level. The first and third terms can become zero if $\hbar$ approaches zero, provided that the other geometrical quantities such as $(\nabla F)^2$ do not cancel $\hbar$. As for the second term, on the other hand, $\hbar$ on the right-hand side has been canceled by $1/\hbar$, which showed up in the phase factor. Thus the smallness of the Planck constant does not directly warrant that this term is negligible. However, if the stationary phase condition holds such that the phase is smooth, that is,

$$\nabla[S_1(q_t,q_0;t)+q_0p_0-q_1p_1]=0, \tag{5.8}$$

the second term of Eq. (5.7) is simply zero. Conversely, if the stationary phase condition is not fulfilled, the error arising from this term must be very large in the order of $\hbar^0$.

Finally, in case of the SADF,

$$\Delta C(t)=\frac{i\hbar}{2}\int dq_t\,F^*(q_t,0)[\nabla^2 F(q_t(q_0,p_0),t)]$$
$$\times\exp\left(\frac{i}{\hbar}[S_1(q_t,q_0;t)+q_0p_0-q_tp_0]\right), \tag{5.9}$$

the above argument can apply equally well, since the stationary phase condition is satisfied as in Eq. (5.5), although the dominant trajectories are not necessarily periodic orbits. Thus if the initial $F(q,0)$ is smooth enough, and if the integration of Eq. (5.9) is performed so as to reproduce the stationary phase situation well, the accuracy of the ADF is conceived to be good as well, which is in accord with our numerical observations made above. We have thus theoretically identified a qualitative domain where our semiclassical scheme can be valid. Together with the numerical study made in Sec. IV, we have shown how efficiently the ADF can work as long as the appropriate applications are made.

VI. CONCLUDING REMARKS

We have presented a semiclassical framework based on the Maslov-type wave packets, the theoretical hierarchy of which lies below or is equal to the level of the standard semiclassical approximation of the Feynman kernel. It includes various levels of approximation, the semiclassical Feynman kernel being the most accurate and time-consuming extreme among them. Another extreme on the other end is the single action-decomposed function, which is a little less accurate but has the fastest convergence in the representation with use of classical trajectories. In fact, it has been shown numerically that a SADF based on an appropriately selected initial wave function, that is, a smooth wave function, can reproduce sufficiently accurate quantum energy spectra from the Fourier transform of the autocorrelation function with far fewer classical trajectories than required by the Feynman kernel. This implies that the SADF and its proximity are quite promising in describing vibrational spectra of relatively large molecules. An application of the present method is in fact under way for a several-atom system.

Finally we would like to stress that the ADF theory is

useful in practical applications but also in exploring the quantum-classical limit of a wave function. For instance, we have found that negative spurious spectra can arise for a positive potential in the domain where the semiclassical theory is not valid. By analyzing those crude cases, one can comprehend a feature of quantum mechanics that to our knowledge has not been shown before. We will report this aspect in the succeeding paper [20].

ACKNOWLEDGMENT

This work was supported in part by a Grant-in-Aid from the Ministry of Education, Science, and Culture of Japan.

APPENDIX: PROOF OF THE SEMICLASSICAL ORTHONORMALITY OF SADF'S

Action-decomposed functions (ADF's) characterized by different initial momenta p_i and p_j are orthonormalized to each other in the lowest-order of $\hbar$ such that

$$\int \Psi^*_{p_i}(q,t)\Psi_{p_j}(q,t)=\begin{cases}1 & \text{if } p_i=p_j\\ O(\hbar^N) & \text{otherwise.}\end{cases} \tag{A1}$$

Substituting the semiclassical expressions for Ψ_{p_i} and Ψ_{p_j}

$$\Psi_p(q,t)=\int dq_t\,\delta(q-q_t)F(q_t,t)\exp\left[\frac{i}{\hbar}S_2(q_t,p_0;t)\right], \tag{A2}$$

we have (neglecting the Maslov index)

$$\int \Psi^*_{p_i}(q,t)\Psi_{p_j}(q,t) = \int dq_t F^*(q_t,t)F(q_t,t) \times\exp\left[\frac{i}{\hbar}\{-S_2(q_t,p_i;t)+S_2(q_t,p_j;t)\}\right]. \tag{A3}$$

Here two different families of classical trajectories are to be considered, namely, the families of classical trajectories which start with an initial momentum p_i (p_j) at $t=0$ and arrives at q_t at time t. In the limit of $\hbar\to 0$, the exponential term oscillates so rapidly that only the trajectories that make the phase stationary as

$$-\frac{\partial S_2(q_t,p_i;t)}{\partial q_t}+\frac{\partial S_2(q_t,p_j;t)}{\partial q_t}=0 \tag{A4}$$

can contribute to the integral, which simply implies

$$p_t(q_t,p_i)=p_t(q_t,p_j). \tag{A5}$$

This, in turn, requires directly that

$$p_i=p_j. \tag{A6}$$

All the other trajectories make contributions to the integral in the order of $O(\hbar^N)$ due to the Riemann-Lebesgue lemma. We thus have seen the semiclassical orthogonality.

On the other hand, if $p_i=p_j$, we observe

$$\int \Psi^*_{p_i}(q,t)\Psi_{p_j}(q,t)dq=\int dq_t F^*(q_t,t)F(q_t,t), \tag{A7}$$

while we have already had

$$F(q_t,t)=F(q_0,0)\left|\frac{\partial q_t}{\partial q_0}\right|^{-1/2}\exp\left[-\frac{i\pi M}{2}\right], \tag{A8}$$

which brings about a normalization

$$\int \Psi^*_{p_i}(q,t)\Psi_{p_i}(q,t)dq=\int F^*(q_0,0)F(q_0,0)dq_0=1. \tag{A9}$$

This completes the proof.

[1] M. V. Berry and K. E. Mount, Rep. Prog. Phys. **35**, 315 (1972).

[2] L. S. Schulman, *Technique and Applications of Path Integration* (Wiley, New York, 1981).

[3] V. P. Maslov and M. V. Feodoriuk, *Semi-Classical Approximation in Quantum Mechanics* (Reidel, Dordrecht, 1981).

[4] M. S. Child, *Semiclassical Mechanics with Molecular Approximations* (Clarendon, Oxford, 1991).

[5] P. Gaspard, D. Alonso, and I. Burghardt, Adv. Chem. Phys. **90**, 105 (1995).

[6] L. G. Yaffe, Rev. Mod. Phys. **54**, 407 (1982).

[7] R. G. Littlejohn, Phys. Rep. **138**, 193 (1986); J. Stat. Phys. **68**, 7 (1992).

[8] S. K. Knudson, J. B. Delos, and B. Bloom, J. Chem. Phys. **83**, 5703 (1985); J. B. Delos, Adv. Chem. Phys. **65**, 161 (1986).

[9] K. Takatsuka and A. Inoue, Phys. Rev. Lett. **78**, 1404 (1997).

[10] H. Goldstein, *Classical Mechanics* (Addison-Wesley, New York, 1980).

[11] J. H. Van Vleck, Proc. Natl. Acad. Sci. USA **14**, 178 (1928).

[12] W. H. Miller, Adv. Chem. Phys. **25**, 69 (1974).

[13] (a) E. J. Heller, J. Chem. Phys. **94**, 2723 (1990); (b) M. A. Sepulveda and E. J. Heller, *ibid.***101**, 8004 (1994); (c) G. Campolieti and P. Brumer, Phys. Rev. A **50**, 997 (1994); D. Provost and P. Brumer, Phys. Rev. Lett. **74**, 250 (1995); (d) K. G. Kay, J. Chem. Phys. **100**, 4377 (1994); *ibid.***100**, 4432 (1994).

[14] A. Messiah, *Quantum Mechanics* (Wiley, New York, 1960).

[15] K. Takatsuka, Phys. Rev. Lett. **61**, 503 (1988); Phys. Rev. A **39**, 5961 (1989); **45**, 4326 (1992).

[16] J. R. Klauder and B.-O. Slagerstam, *Coherent States* (World Scientific, Singapore, 1985).

[17] E. J. Heller, J. Chem. Phys. **62**, 1544 (1975); **65**, 4979 (1976).

[18] W. H. Press, S. A. Teukolsky, W. T. Vetterling, and B. P. Flannery, *Numerical Recipes* (Cambridge University Press, Cambridge, 1992).

[19] K. Takatsuka and H. Nakamura, J. Chem. Phys. **82**, 2573 (1985); **83**, 3491 (1985); **85**, 5779 (1986).
[20] A. Inoue-Ushiyama and K. Takatsuka (unpublished).
[21] V. I. Arnold, *Mathematical Methods of Classical Mechanics* (Springer, Berlin, 1979).
[22] M. C. Gutzwiller, J. Math. Phys. **11**, 1791 (1970); **12**, 343 (1971).
[23] M. C. Gutzwiller, *Chaos in Classical and Quantum Mechanics* (Springer, Berlin, 1990).